

Guiding centre simulation of neoclassical impurity transport in the pedestal region of a tokamak

A. Bergmann

Max-Planck-Institut für Plasmaphysik, 85748 Garching, Germany

The neoclassical transport of trace impurities in the pedestal region of a tokamak plasma is studied with guiding centre particle simulations, employing the HAGIS code [1] with a Monte Carlo collisions model [2]. The simulations are done in two steps: First, the density and temperature profiles and the parallel velocity of the main ions (D) are obtained from a simulation with D-D collisions. Then for each of various impurity species a simulation is made including only collisions between the impurity ions and the main ions. An equilibrium with X-point is used and the simulations cover the edge region inside the separatrix with closed flux surfaces. The electric potential is assumed as a flux function. HAGIS is a δf code, the guiding center distribution function is split into f_0 and δf , where only δf is represented by marker particles. The evolution of the weights for δf is calculated from the change of f_0 along the orbits and the contribution of the collisions. f_0 is chosen so that it is invariant under the collisions. In the simulations of the main ions f_0 is a Maxwellian centered at $v = 0$, and in the impurity simulations f_0 is a Maxwellian (with the same temperature as the main ions) centered around the parallel velocity $u_{i\parallel}$ of the main ions. The simulations are made in the lab frame, but the effect of the impurity-ion collisions is calculated in a frame moving with $u_{i\parallel}$, approximating the main ion distribution function by a Maxwellian around $u_{i\parallel}$. Several cases have been studied, here results for one case are presented. The profiles of the main ion density, temperature and parallel velocity are shown in Fig. 1. The toroidal velocities and densities of four impurity species at four poloidal angles ($\theta = 0$ (low field side midplane), $\theta = \pi$ (h.f.s. midpl.), $\theta = \pm\pi/2$ (top, bottom)) are shown in Fig. 2. For low and medium Z impurities there are the well-known in-out asym-

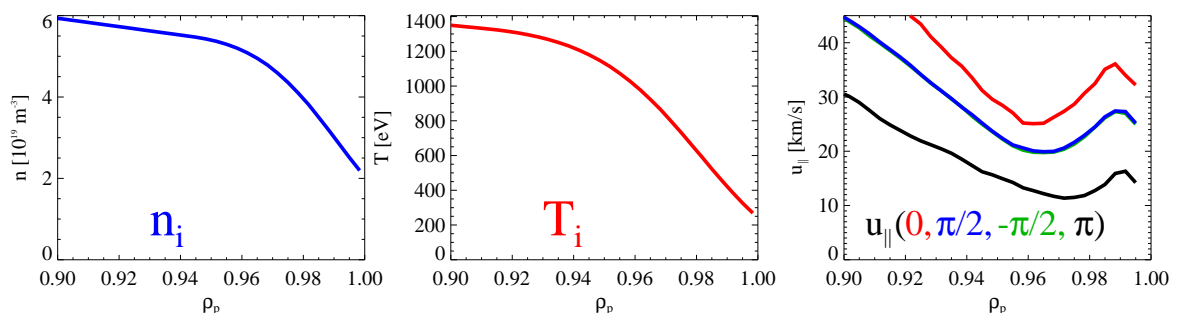


Fig. 1: Deuterium density, temperature and parallel velocity (at four pol. angles).

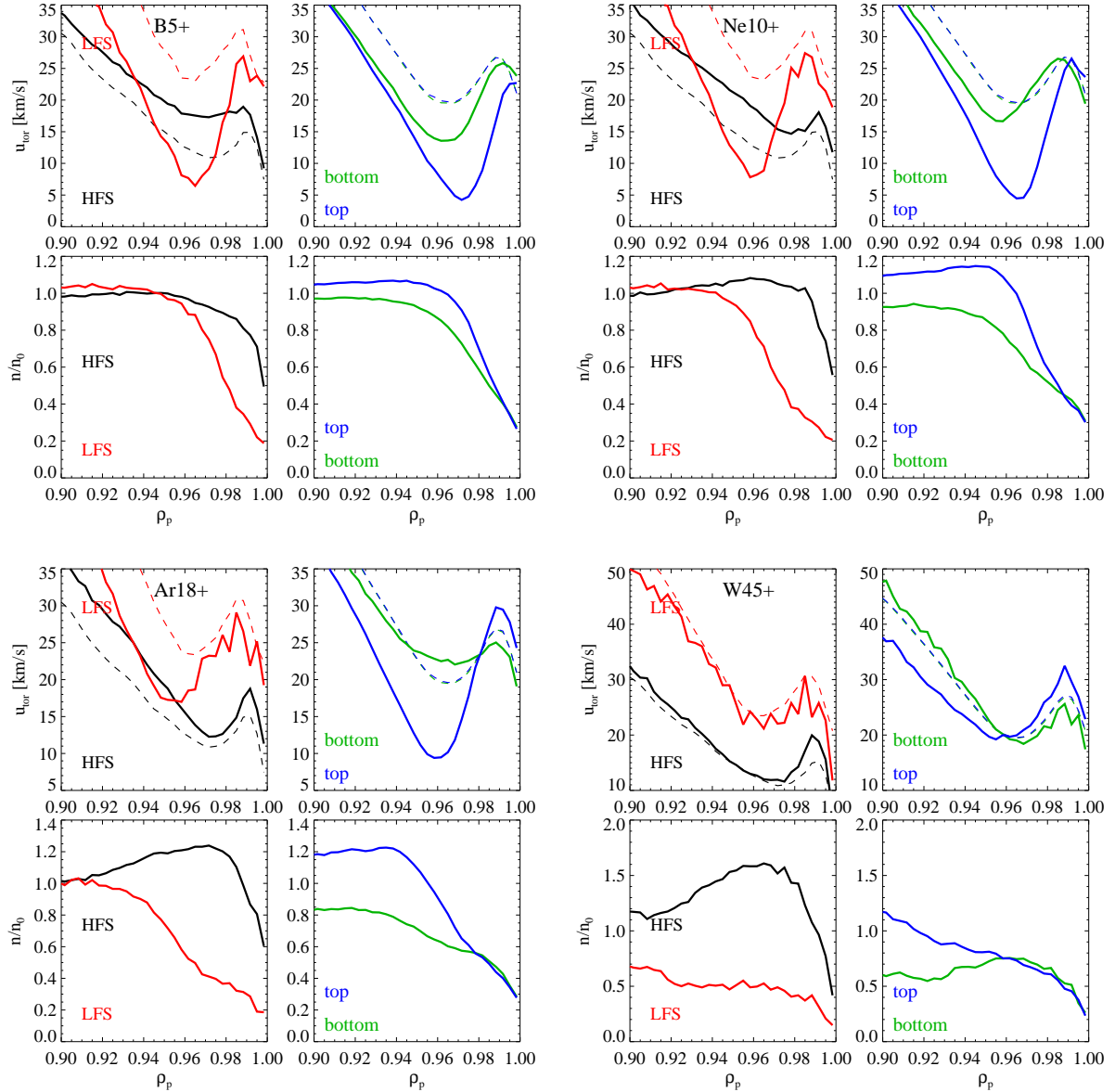


Fig. 2: Toroidal velocity and density at poloidal angles $\theta = 0$ (LFS), $\theta = \pi$ (HFS), $\theta = \pi/2$ (top) and $\theta = 3\pi/2$ (bottom) for impurities B5+, Ne10+, Ar18+ and W45+.

metries of density and toroidal velocities. While the in-out density asymmetry increases with higher charge number, the velocities are closer to the main ion velocities due to the strong friction. In addition to in-out asymmetries there are also strong up-down asymmetries of the toroidal velocity and the density. The full poloidal variation of toroidal velocity and density is shown in Fig. 3. For the low Z impurities the minimum of the toroidal velocity is at the top and the maximum is at the upper h.f.s. For W45+ the velocity is close to that of the main ions. The velocity variation agrees with the neoclassical expression with the poloidal variation of density and velocity included. In the outer pedestal region the in-out density ratio (shown in Fig. 4) is close to $(B(\pi)/B(0))^2$ for which the friction force vanishes [3]. The up-down density asymmetry is needed for the radial particle transport. From the expression for the grad B and curvature

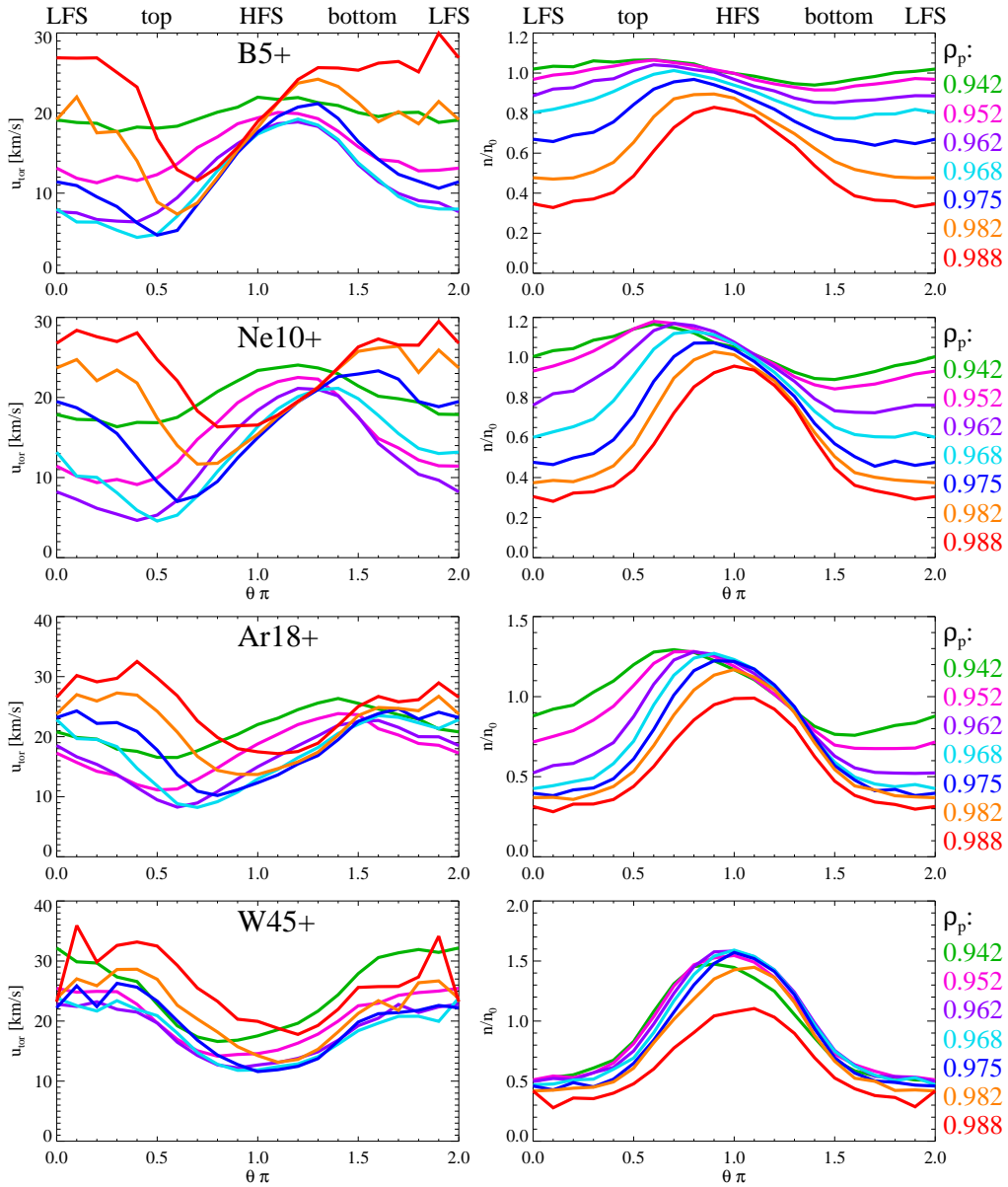


Fig. 3: Poloidal variation of tor. velocity and density for B5+, Ne10+, Ar18+ and W45+.

drift we get with $p_{\parallel} = p_{\perp} = p$

$$\int (v_d \cdot \nabla \psi) f d^3v = \frac{B \times \nabla B \cdot \nabla \psi}{ZeB^3} \int \left(\frac{m}{2} v_{\perp}^2 + m v_{\parallel}^2 \right) f d^3v = -RB_t \frac{\partial B}{\partial \theta} \frac{B \cdot \nabla \theta}{ZeB^3} 2p(1 + M^2)$$

where $M^2 = mu_{\parallel}^2/2T$. Since $\partial B/\partial \theta$ is up-down asymmetric, whereas B and M are in-out asymmetric, we need an up-down asymmetric density for a finite radial transport (with $T \approx \text{const.}$). In Fig. 5 the up-down density ratio is compared with the radial flux divided by the density (effective radial velocity). The collisional radial impurity flux is calculated by summing up the collisional changes of the parallel momentum making use of the neoclassical flux friction relation, $\langle \Gamma_r \rangle = -\langle R_{\parallel}/ZeB_p \rangle$, which holds in steady state (B_p : poloidal magnetic field). At a fixed

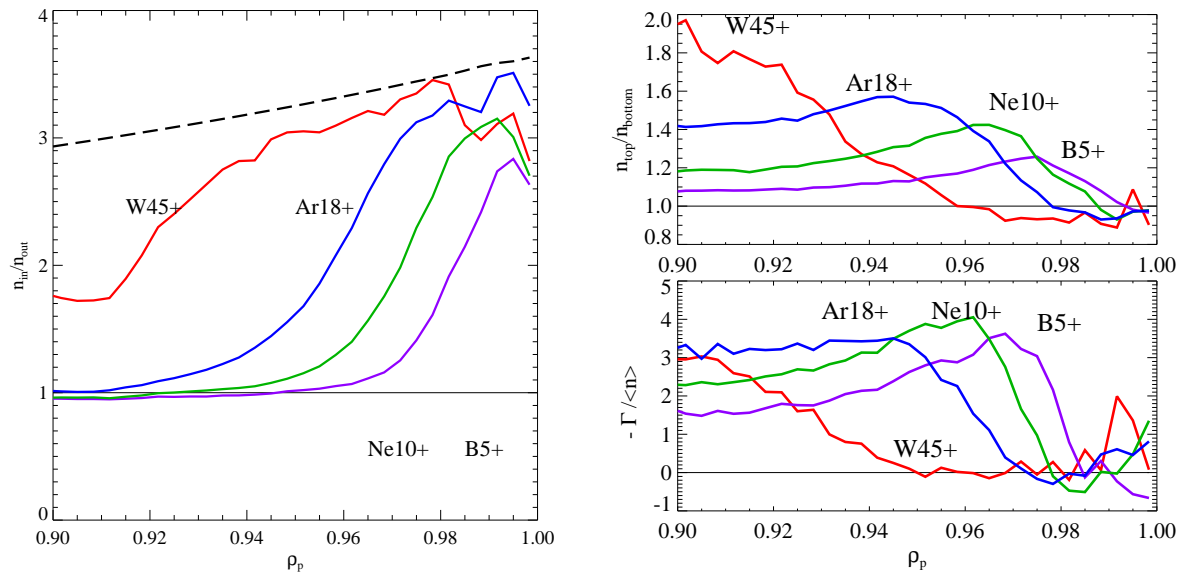


Fig. 4 (left): In-out density ratio and $(B(\pi)/B(0))^2$ (dashed). Fig. 5 (right): Up-down density ratio and radial flux divided by the density. Both graphs with data for B5+, Ne10+, Ar18+ and W45+.

radius the transport decreases with increasing Z , but the maximum increases as to be expected from the analytic theory (temperature screening is not included in our simulation),

$$\frac{\langle \Gamma_{Zr} \rangle}{\langle n_Z \rangle} = -Z \left\langle \frac{B_I^2}{B_p^2} \right\rangle \frac{v_{ii}}{\omega_{ci}} \frac{\rho_i}{L_p} v_{Ti} \left(\left(\left\langle \frac{n_Z}{B^2} \right\rangle - \left\langle \frac{B^2}{n_Z} \right\rangle^{-1} \right) \frac{\langle B^2 \rangle}{\langle n_Z \rangle} \right)$$

Compared to that the transport is reduced in the pedestal region (Fig. 6).

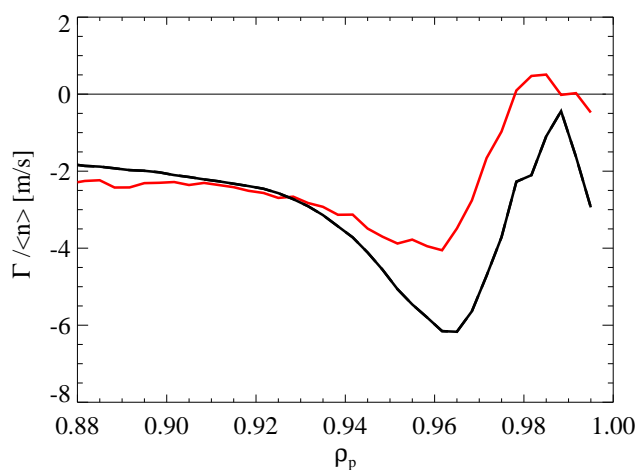


Fig. 6: Effective radial velocity compared to analytic theory.

- [1] S.D. Pinches *et al.*, *Comp. Phys. Comm.* 111, 133 (1998)
- [2] A. Bergmann, E. Poli, A. Peeters, *Phys. Plasmas* 16, 092507 (2009)
- [3] T. Fülöp and P. Helander, *Phys. Plasmas* 6, 3066 (1999)